Title
Hydrologic and topographic variability modulate channel change in mountain rivers

Journal
Journal of Hydrology, 510

ISSN
00221694

Authors
Brown, Rocko A
Pasternack, Gregory B

Publication Date
2014-03-01

DOI
10.1016/j.jhydrol.2013.12.048

Peer reviewed

Title: Hydrologic and Topographic Variability Modulate Channel Change in Mountain Rivers

Authors:

Rocko A. Brown* and Gregory B. Pasternack

Key words: topography; hydrology; channel change; flow convergence; topographic change detection; mountain rivers; process blending

Department of Land, Air, and Water Resources, University of California, One Shields Avenue, Davis, CA 95616, USA.

*Corresponding author. Tel.: (510) 333-5131; E-mail:rokbrown@ucdavis.edu

Abstract

The relationships between flow hydrology, topography, and channel change in mountain rivers is important to understanding landscape evolution, the structure and persistence of aquatic habitat, and also the physiochemical cycling of upstream derived organic and inorganic materials. There is a paucity of detailed studies that analyze the joint roles of hydrology and topography in controlling multiple mechanisms of channel change in mountain rivers. In this study, gravel and cobble channel change in a bedrock river canyon were analyzed in light of a controlled yet natural experiment where 4,491 metric tonnes of rounded gravel and cobble was augmented below a sediment-barrier dam in a 1,200 m long mountain river reach that had no prior sources of rounded gravel or cobble and still experiences floods above the bankfull discharge. The overall study goal was to investigate how flow hydrology can modulate multiple channel change processes depending on the topographic features engaged by the flow. Channel change was assessed via differencing of high resolution repeat topographic and bathymetric surveys, along with cm-scale aerial photography post injection. Statistical tests used to implicate topographic feature-specific mechanisms of channel change that vary with discharge included analyzing geomorphic covariance structures of flow dependent width, bed elevation, and channel change as well as autocorrelation of flow width spatial series. Stage dependent topographic steering was inferred from associations of erosion and deposition with changes in 2D model derived flow directions at multiple discharges. A variety of mechanisms of channel change were qualitatively and quantitatively confirmed including particle hiding, topographic steering, eddying, and flow convergence. No single mechanism explained the observed patterns of channel change but rather it is thought that process-blending occurs, as modulated by the interactions of flow hydrology with complex topography. Results from this study suggest that

both existing channel boundary variability and input hydrologic variability work together to create hydrodynamic spatial patterns that control the fate and transport of sediments in mountain rivers and ultimately their spatial structure.

1 Introduction

Mountain rivers are important corridors linking upland and lowland environments as well as mediating the supply, transport, and storage of organic and inorganic materials (Hynes, 1970; Wohl, 2000). Further, mountain rivers are often confined by immobile topographic features such as bedrock and large boulders with channel gradients commonly exceeding 1% (Grant, 1990; Grant and Swanson, 1995; Wohl, 2000; Wohl et al., 2004). This leads to these types of rivers having steep hydraulic rating curves initiating rapid transport of smaller sand and gravel fractions within a larger structural matrix formed by large, century scale floods nested within an even larger geological context (Wohl, 2000; Fryirs and Brierely, 2010). A plethora of studies have sought to understand the complex feedbacks of channel topography, flow-dependent hydrodynamics and channel change of the more mobile gravel fraction, but usually these studies are limited to the morphological-unit (i.e., 10^0-10^1 channel widths) spatial scale of analyses (e.g., Rathburn and Wohl, 2003; Wohl and Legleiter, 2003; Hassan and Woodsmith, 2005; MacVicar and Roy, 2007). Contrasting these morphological-unit-scale studies is an emerging view in fluvial geomorphology that rivers are systems with multiple scales of variability (Fonstad and Marcus, 2010; White et al., 2010; Carbonneau et al., 2012), necessitating the study of larger areas while retaining the same level of detail. While the importance of mountain rivers within fluvial systems is understood, there is still a gap in how multiple scale-dependent mechanisms of channel change relate to topography and flow hydrology in mountain river reaches. In this article a diverse array of state-of-the-art methods of fluvial geomorphic inquiry, such as two-dimensional (2D) modeling, spatially explicit topographic change detection with uncertainty analysis, and geospatial/statistical analyses were coupled with pre- and post- experiment datasets to evaluate the relationship between channel change, river corridor topography and hydrology.

1.1 Linkages among channel change, topography, and hydrology in mountain rivers

The interplay between antecedent topography, boundary resistance, sediment supply, and flow stage and discharge produce a variety hydrodynamic and sediment transport processes that can mediate channel change in rivers. The topography of mountain rivers, however, consist of a mosaic of landforms (Montgomery and Buffington, 1997; Wohl and Merritt, 2001) comprised of relatively immobile materials such as coarse grained alluvium and bedrock, upon which finer gravel, cobble, and sand fractions interact (Cenderelli and Cluer, 1998). Variations in mobility of existing and incoming material, along with local bedrock geology, leads channel topography in these types of rivers to be layered with multiple scales of topographic variability (O'Connor et al., 1986; Fryirs and Brierely, 2010). Because of the diversity of topographic features a variety of depositional and erosive forms are present, each occurring from a combination of channel change mechanisms.

Some of the most commonly reported mechanisms of channel change in mountain rivers are particle trapping (Brayshaw, 1985; Grant et al., 1990), topographic steering (Whiting and Dietrich, 1991; MacWilliams et al., 2006), eddying (Lisle, 1986; Rathburn and Wohl, 2003; Woodsmith and Hassan, 2005; Thompson et al., 2009), flow convergence (MacWilliams et al., 2006; Harrison and Keller, 2007; Thompson, 2011), and backwatering from broader scale valley changes in flow width (Cenderelli and Cluer, 1998; Howard and Dolan, 1981; White et al., 2010) large debris jams (Howard and Dolan, 1981; Montgomery et al., 2003), or at tributary junctions

(Table 1). Each of these mechanisms is associated with specific scales of topographic variability and may act within different ranges of the daily flow exceedance hydrology. At all channel mobilizing flows selective deposition through particle trapping can occur upstream and within non-mobile topographic and grain scale features < 10^{-1} channel widths, such as bedrock fractures, outcrops, individual boulders and large cobbles, as smaller bedload particles in motion will accumulate upstream of these features or within interstitial pockets (Brayshaw, 1985; Grant et al., 1990). Topographic steering occurs when water flow direction is controlled by immobile topographic features such as boulders, bedrock, and alluvial deposits. Material in transport can be steered by the main flow direction and effectively pushed into immobile topographic features creating depositional forms, or deposit due to particle trapping. For flows equal to or greater than bankfull (e.g. <50% daily flow exceedance) morphological-unit scale features can induce channel curvature that may create positive feedbacks between topographic steering of the flow field, secondary flow circulation, inward (i.e. towards the origin of curvature) deposition due to cross channel variations in sediment competence, and inward transport at the bed (Whiting and Dietrich, 1991; MacWilliams et al., 2006). Although poorly studied, flow directions in rivers often change with increasing discharge, meaning that a variety of complex responses can occur between discharge, flow direction, sediment transport and channel change (e.g., Rathburn and Wohl, 2003). Flow convergence is the stage-dependent funneling of flow from riffles to pools, mediated by variations in flow width and bed elevation (MacWilliams et al., 2006; Harrison and Keller, 2007; Thompson,2011). The mechanism posits that for undulating bed topography consisting of a riffle and pool at low flows (e.g. >90% daily flow exceedance) peak velocity and shear stress occur over the riffle. At bankfull flows and higher (e.g. <50% daily flow exceedance) constrictions adjacent to the pool can create narrow jets of lateral and vertical flow convergence that enhance turbulence and bed shear stresses that form and maintain pools. Above the constriction a backwater can form, leading to deposition and maintenance of the upstream riffle. Flow convergence can be induced through hydraulic-unit to morphologic unit scale (10^{-1}-10^{1} channel widths) topographic features such as gravel bars (MacWilliams et al., 2006; Sawyer et al., 2010) large boulders (Harrison and Keller, 2007), large streamwood (Buffington et al., 2002) and bedrock outcrops (Lisle, 1986; Wohl and Legleiter, 2003; Woodsmith and Hassan, 2005; MacVicar and Roy, 2007). Related to flow convergence, recirculating eddies below channel constrictions can also cause deposition of finer materials in transport (Lisle, 1986; Rathburn and Wohl, 2003; Woodsmith and Hassan, 2005; Thompson et al., 2009). Moreover, larger scale changes in valley width at expansion zones associated with morphological unit and reach scales are thought to promote depositional features from backwatering that may promote deposition and increase bed relief, which in turn can provide positive feedbacks with the prior scale-dependent sediment deposition mechanisms mentioned earlier (Cenderelli and Cluer, 1998; Howard and Dolan, 1981; White et al., 2010), but the effect of these features is only prominent at flood discharges (e.g. <10% daily flow exceedance). While these mechanisms have ranges of spatial scales associated with topographic variability, the flow stage also mediates how each one of these features is activated into contributing to channel change.

The goal of this study was to investigate the hydrologic modulation of scale-dependent topographic features that control channel change in mountain rivers. A unique opportunity to consider this problem was presented when 4,491 metric tonnes of gravel ranging from 6-128 mm was quickly injected directly below a dam for spawning habitat rehabilitation (Pasternack et al., 2010) in a mountain river with no other sources of gravel/cobble sediment supply and virtually no storage of those sizes of river-rounded alluvium in the system. Several tests are employed to investigate the hydrologic modulation of process blending of multiple channel change mechanisms through the activation of complex boundary topography (Table 2). Channel change was inferred from topographic change detection (TCD) analyses of pre and post gravel injection digital elevation models (DEMs), ground based observations, high resolution kite-blimp photography. This provided qualitative and quantitative evidence of where channel change occurred after the injection. Of the mechanisms discussed in Table 1 only topographic steering, flow convergence, and eddying are explored here, but particle trapping was examined qualitatively. Valley scale backwatering could not be investigated because the flow record during the study period did not allow for it to be assessed explicitly, but inferences are made from prior flood observations. Because different processes can occur simultaneously, several statistical analyses were employed to test associations among topographic change, serial covariance of flow dependent channel geometry, and changes in flow direction to assess the role of channel topography on the spatial patterns of channel change.

2 Study Reach

The location for this experiment was the Englebright Dam Reach (EDR) of the Yuba River located below Englebright Dam in California, USA (Fig.1 a). This reach has been studied and extensively documented by Pasternack et al. (2010); herein only information relevant to this study is recounted. The EDR is a 1,200-m long mountain river reach with an overall slope of 0.31% and an existing substrate of bedrock, large cobbles (e.g. >250mm) pre-dating dam construction, angular shot rock (>0.5m) and boulders (>1m), with the last two stemming from natural landslides of shallow, weathered bedrock and bedrock blasting of canyon walls during dam construction circa 1940. The bankfull discharge and width have been estimated by prior authors to be 141.5 m^3/s and 59 m, respectively (Wyrick and Pasternack, 2012). Numerous bedrock outcrops exist along the channel banks, ranging 10^{-1}-10^{2} channel widths (Fig.1). Bedrock canyon walls confine the river, though there are two cobble/boulder bars at canyon expansions. The upstream expansion consists of a cobble bar on river left with a rapid centered on station 655 that impinges into a bedrock outcrop (Fig.1 a,c). The downstream expansion is the largest in the reach and has a very large cobble/boulder bar on river right that extends to the downstream study limits (Fig.1 a,b). This alluvial bar has been depositional despite several large floods and has subsequently coarsened due to the lack of gravel in the river, consisting of large boulders and angular shot rock (Pasternack et al., 2010). A large 5 m high by 3 m wide boulder is also present on river right at station 580. Centered at station 200 there is also a riffle that has persisted since 1908 (Pasternack et al., 2010), with a pool located above and below centered at stations 290 and 90, respectively. There are no tributaries in the study reach, but Deer Creek is located just below the study limit.

A gravel injection project took place immediately downstream of the second powerhouse located below Englebright Dam (Fig. 1). A total of 4,491 metric tonnes of gravel/cobble sediments ranging from 16 to 128 mm was sluiced into the river as weather permitted during November 2010 to January 2011 when discharges were approximately 1/3 to 1/2 of the bankfull discharge. Bathymetric mapping of the injected sediments within the river commenced immediately after injection on January 17th, 2011. While the study reach is in a regulated river, flows above 117 m^3/s still overtop the dam so natural aspects of the hydrograph are still retained such that the reach still experiences large floods capable of considerable topographic change

(Pasternack et al., 2010). Between the gravel injection in January of 2011 and May of 2011 there were several flood events ranging from 226 to 538 m^3/s that were well above the bankfull discharge of 141.5 m^3/s (Fig. 2). The first two events were rain-driven with sharp peaks and gradual receding limbs, while the remaining events were driven by a mixture of rain and snow with more gradual rising and receding limbs.

3 Experimental Design

To test the study hypotheses several field and numerical tools common to modern fluvial geomorphic inquiry were coupled with new analyses of channel geometry and topographic change. The methods are detailed in section 4 below, but an overview is provided here to put them in the context of the whole experimental design. First, bathymetric and topographic channel surveys before and after gravel/cobble injection were conducted between flood seasons and used to create pre- and post-season DEMs. Second, spatially explicit topographic change detection with uncertainty analysis (Carley et al., 2012) was used on the DEMs to map patterns of statistically significant topographic changes caused by the floods. Third, a 2D hydrodynamic model was validated and used to simulate the spatial patterns of wetted width, depth, velocity magnitude, and velocity direction for discharges of 28.3, 141.5, and 242.8 m^3/s, representative of baseflow, bankfull, and flood discharges, respectively. These instantaneous flows represented daily flow exceedance probabilities of 0.1, 56, and 99% during the time period between the injection and the post flood survey and 45, 82, and 99% daily flow exceedance probabilities (Wyrick and Pasternack, 2012). Finally, statistical analyses tested associations among topographic change, serial covariance of flow dependent channel geometry, changes in flow direction, and flow-dependent changes in the autocorrelation of flow widths.

To evaluate the mechanisms responsible for channel change in the field-scale experiment, both qualitative description and quantitative hypothesis testing were used (Table 2). First, a topographic change detection (TCD) analysis was performed to generate a data set representing statistically significant areas of channel change. This was paired with ground observations and high-resolution kite-blimp photography to ground more sophisticated analyses with standard geomorphic observations. Then, using the TCD data three different quantitative tests were used to assess how various scales of topography and hydrology control channel change.

The first test was a spatial series covariance of flow widths and bed elevation versus topographic change for the three discharges modeled, aimed at understanding morphological unit to reach scale channel change associated with flow convergence and changes in flow competence. This test evaluated whether channel change was spatially correlated with the standardized residuals of flow width or bed elevation, while the latter was detrended. For example, by simple flow continuity deposition may preferentially occur in wider areas that have lower average velocities and erosion in narrower areas where velocities would be relatively higher. Using this test on multiple flows captures the hydrodynamic activation of topographic features that control channel width from low to flood flows. Changes in flow width were hypothesized to control patterns of channel change, because of the linkages between flow-dependent width and flow convergence (Table 1). Before correlating these variables with channel change, first they were correlated with the peak velocity to understand whether one or the other was associated with discharge.

The second test was a correlation of topographic change versus the change in 2D model derived flow direction for each model domain point relative to the main flow direction for the same three discharges. In this case, this test evaluated whether flow direction changes control patterns of topographic change and how this changes with flow. Channel change was hypothesized to correlate strongly with the main flow path and thus be strongly associated with minor deviations (e.g. < 30 degrees) in flow direction. This relationship was hypothesized to peak at the flood discharge, but that as flow decreases a wider domain of flow direction changes will be associated with channel change, specifically deposition. The reasoning is that higher discharges push gravel into obstructions and topographic features and that these frontal deposits in turn steer flow paths at the base flow.

The final test analyzed the autocorrelation of the flow width series to infer the spatial scales of correlations and how these change with discharge. As discharge increases the spatial correlations of flow width was hypothesized to also increase, implying that broader scale features dominates these spatial series and ultimately, channel change. Together these tests along with a qualitative assessment of channel change, topography and flow direction were used to assess the role of topographic and hydrologic variability on controlling channel change.

4 Methods

The methods for this study were detailed in a technical report (Brown and Pasternack, 2012) available to the public online (http://pasternack.ucdavis.edu/research/projects/river-rehab/cobblegravel-injection/), so herein methods for data collection, 2D modeling, topographic change detection, and data analysis are briefly summarized.

4.1 Topographic and bathymetric mapping

Topographic maps were made in 2007 before the injection (Pasternack et al., 2010) and approximately 10 months after the gravel injection (Pasternack et al., 2010; Brown and Pasternack, 2012). Bathymetric observations were made by boat using a single-beam echosounder coupled to a real-time kinematic global positioning system (RTK GPS). Wadable bathymetry and the terrestrial river corridor were mapped at the outset using a robotic total station. Valley walls were also mapped at the outset, but using a reflectorless total station. For the most distal hillsides and bedrock walls not very relevant to this study but necessary to complete the map, elevations were taken from a 1999 DEM made using photogrammetry by Ayres Associates. The point density for the pre injection topography was 1.6 points per square meter, while the post injection point density was 0.8 points per square meter.

4.2 2D modeling

2Dmodeling was done using Surface water Modeling System 10.1 for computational mesh preparation and Sedimentation and River Hydraulics- Two-Dimensional (SRH-2D) for solving the depth-averaged St. Venant equations. Model outputs include point based water surface elevation, water depth, depth-averaged velocity components, depth-averaged water speed, Froude number, and shear stress. For more information, see http://www.usbr.gov/pmts/sediment/model/srh2d/index.html as well as the 2D modeling textbook by Pasternack (2011). Three computational meshes with ~ 1 m internodal spacing were made to span 2.5 orders of magnitude of flow (e.g. apprximately 19.8 to 2830 m^3/s). Discharge data was obtained from the U.S. Geological Survey gaging station (#11418000) located in the model domain. Turbulence closure was achieved with a k-ε model. Exit water surface elevations were measured periodically, while those for unmeasurable higher flows were estimated by extrapolating the values from the nearby gage downstream ~ 730 m on the basis of observed water surface slopes. The model was validated at six different flows ranging between 23.3 and 27.3 m^3/s for mass conservation, water surface elevation, velocity magnitude, and flow direction. For brevity, the validation for a flow of 24.1 m^3/s is reported herein (see Brown and Pasternack, 2012 for full details). Mass conservation assessments were done for all modeled discharges that compared inflow versus outflow and the error was < 0.01%. For water surface elevation the absolute deviation from measured and modeled values ranged from 0.008 to 0.076 m with 50% of the deviations less than 0.03 m. The coefficient of determination for modeled versus measured velocity magnitude was 0.76. Unsigned errors (e.g. absolute value of both positive and negative flow direction change) for velocities > 0.6 m/s were 11%, while those < 0.6 m/s were 21%. For flow direction the average and median signed angle deviations were 1.3˚ and 1.1˚, respectively, while the same values for unsigned deviations were 5.9˚ and 4.8˚, respectively. Overall, the 2D model was validated very thoroughly and met common standards, so it was deemed a legitimate tool for assessing hydrodynamic patterns capable of controlling channel change.

4.3 Topographic change detection

Topographic change detection (TCD) is an emerging tool in fluvial geomorphology (Wheaton et al., 2009; 2010; Carley et al., 2012) where a raster grid of topography from one period is subtracted from another with the resulting difference indicating the locations and magnitudes of landform change. Modern topographic change detection differs from simple

DEM differencing in that a spatially distributed statistical significance can be associated with each topographic data set that explicitly incorporates instrument and interpolation errors along with intrinsic surface variability (Milan et al., 2011). In this study the Carley et al. (2012) method of accounting for uncertainty with geomorphic change detection was utilized to perform topographic change detection. This method is based on the idea that locations where there is a lot of topographic variation in the raw point data for a topographic map are the ones that are most uncertain. Because of the significant role of the rapid downstream of the USGS gaging station in serving as a topographic control on channel hydraulics, the EDR was divided into two sections- one upstream and one downstream of the rapid- for TCD analysis (Fig. 1). Each section of the canyon was evaluated for change in the epoch from the date of last survey of the baseline map (November, 2007) to the date of the post-floods survey in the dry season (October, 2011). In addition, two intermediate TCD analyses for the upstream zone were performed for i) the baseline DEM and the pre-flood season DEM mapped in January, 2001 and ii) the latter data set and the post-flood DEM. These were meant to account for the addition of injected sediments as well as their export over the flood season. All TCD analyses used 0.9 meter grids and only used statistically significant changes ($p < 0.05$). In addition to the base TCD analysis, histograms of erosion and deposition were produced to infer the modes of channel change although they are only described here for brevity.

4.4 Aerial kite-blimp imagery

Deposits occurring from particle trapping were too thin to detect from the TCD analysis due to the inherent roughness of the pre-injection topography. As an aid for locating deposits from particle trapping, as well as confirming the predicted TCD spatial extents, ~ 5x5-cm^2 resolution aerial imagery was collected with a tethered helium kite-blimp and used along with field observations to map visible new gravel deposits. This was possible because the injected sediments were brighter and rounder than the existing substrate. Imagery was taken in autumn 2012 with a 14.7 megapixel digital camera (Canon Powershot SD990 IS). Agisoft Photoscan was used to mosaic images and then the mosaic was georectified in ArcGIS using surveyed aerial targets.

4.5 Data analysis

Once TCD analysis, aerial imagery analysis, and 2D modeling were complete, results were processed to generate data sets tailored to the three tests outlined above in section 3. For geospatial analysis of rivers it is important to recognize that river topography is anisotropic, which precludes the use of Cartesian coordinates in analysis (Merwade et al., 2005). To account for anisotropic variations a centerline needs to be established so that the river can be placed with an orthogonal, curvilinear coordinate system (Smith and McLean, 1984; Leigleiter and Kyriakidis, 2006) that can facilitate analysis relative to the main flow direction of the river. To create a centerline for the curvilinear coordinate system, the product $d_i * v_i$, where $d_i$is the depth and v_i is the velocity at node i in the model domain, was calculated for each grid cell of the depth and velocity model outputs at the bankfull flow of 141.5 m^3/s. Once a grid of dv was made a path was defined along the greatest values going from downstream to upstream (Pasternack, 2011) and this was used as the reference centerline for all further analyses. Finally, the thalweg was stationed every 0.9 m to be consistent with the resolution of the topographic data and the 2D model mesh.

4.5.1 Geomorphic covariance structures and channel change

A geomorphic covariance structure (GCS) is a spatial covariance plot of two standardized geomorphic series, such as bed elevation and channel width, that can be used to infer spatially explicit relationships between variables (Brown et al., submitted). This paragraph explains the types of GCS analyses performed while the latter explains both data extraction and the statistical significance testing employed. For this study, several pairs of GCS's were analyzed. The first GCS analyzed was between the 2D model derived flow width (W_{ij}) and detrended, centerline bed elevation (Z_i), where i indexes the stationing along the thalweg and j indexes discharge, to determine if statistically significant areas were present and how they change with flow discharge. This GCS was compared with the detrended, pre injection topography to relate GCS structure with specific topographic features. Next, this GCS was compared with the patterns of standardized, 2D model derived centerline velocity (V_{ij}) to determine if the GCS structure and velocity signal had similar patterns, and could thus if they could be used to indicate whether flow convergence occurred. This was done to determine if reversals or phasing of V_{ij} occurred, and if this was associated with W_{ij} and/or Z_i. In areas where flow convergence is present it is expected that a reversal or phase shift in the velocity signal will occur between riffle and pool units (Wilkinson et al. 2004; MacWilliams et al., 2006). Bivariate Pearson's correlation coefficients (r) values were also calculated between V_{ij} and W_{ij} and V_{ij} and Z_i to determine if flow width or bed elevation were related to the velocity signal and how that changed with discharge. After establishing a relationship (or lack thereof) between flow width, bed elevation, and peak centerline velocity, an additional GCS analysis was performed with the volume of topographic change associated with each channel thalweg node, and W_{ij} and Z_i to determine if and where either were associated with channel change. This GCS does not explicitly rely on a particular mechanism, but evaluates the role of stage dependent oscillations in flow width and bed elevation in modulating perhaps several mechanisms in controlling channel change. Finally, the bivariate Pearson's correlation coefficients (r) of covariances were calculated between combinations of the channel change,W_{ij}, and Z_i and assessed at the 95% confidence limit to find out if any of them were interdependent.

To perform the above analyses data had to first be extracted and then analyzed statistically. Bed elevation data was sampled along the thalweg as described in Section 4.5. For flow width series, transects were created at each station and clipped by the wetted area polygon for each discharge simulated. The length of each clipped transect with distance along the centerline gives a series of flow width. Similar to the channel-referenced flow direction analysis described above, a spatial series of the volume of topographic change for each stationing node was determined using a nearest point algorithm in ArcGIS 10.1. The GCS between paired series was calculated from detrended, standardized series residuals by the product $x_{std,i} * y_{std,i,}$where the subscript *std* refers to standardized values of two variables x and y at location i along the centerline. To extract series, the thalweg was used to sample bed elevation and flow widths at each 0.9 m spaced node. With regards to the spatial series of flow width and bed elevation only the latter was detrended, because the downstream variation in width was hypothesized a priori to be a controlling factor on topographic change. Next, each series was standardized by the mean and variance of the entire series (Salas et al., 1980) and cross multiplied to yield a series of spatial covariance. To test each standardized series for normality a chi-square test was performed, and all data series were significant ($p = 0.05$). Because the data was standardized, successive increments from 0 indicate increasing significance, analogous to Z-scores. The hypothesis for this test has two parts; (i) there are statistically significant correlations between flow width and channel change and (ii) the correlation strength increases with discharge. Serial correlations of flow width and channel change were assessed at both the the 67% and 95% confidence intervals. Bivariate correlations of each flow specific flow width and channel change population were assessed at the 95% confidence level.

4.5.2 Flow direction change and channel change

To evaluate the relationship between flow-dependent topographic steering and channel change, each channel change cell was associated with the change in 2D model derived flow direction at each model node. Unlike most 2D modeling studies, this study actually validated flow direction, making it suitable for use in geomorphic analysis. A novel approach was used here to analyze the change in flow direction for each 2D model point relative to the channel centerline. Consider the two velocity components of a 2D flow point within the model domain, V_x and V_y, where V_x is the X component and V_y is the Y component of the total resultant velocity vector, V. The two components are related to the total resultant velocity magnitude by $V = \sqrt{V_X^2 + V_Y^2}$ and the direction is determined by the absolute angle, θ, given by $\tan^{-1}\frac{V_y}{V_x}$. This was done for each model output point and also each centerline node yielding the absolute angles, θ_{xy} and θ_s respectively. To determine the angle associated with a Cartesian plane, θ_c, a linear shift was applied depending on which quadrant the point lied in. The shift is 0 degrees for points in quadrant I, 180 degrees for quadrants II and III, and 360 degrees for quadrant VI. To calculate the change in direction of each 2D model point relative to the centerline a nearest point algorithm was used in ArcGIS 10 that determines the centerline node closest to each model point so that the change in direction could be calculated as $\Delta\theta_{cs} = \theta_{xy} - \theta_s$. It follows from Fig. 3 that negative values correspond to flow direction changes in which a flow vector is oriented towards river right and positive values when a flow vector is oriented towards river left. Similarly, negative and positive values greater than 90 degrees correspond to flow vectors that are at the onset of eddying upstream. After rasters of flow direction change were created, each deposition and erosion cell from the TCD analysis was then joined to the associated change in flow direction for each discharge modeled.

Three-dimensional (3D) histograms were created to illustrate relationships between changes in flow direction and channel change. This analysis does not have a traditional statistical test but relies on the qualitative inference of the patterns for each discharge dependent 3D histogram. In the case where flow direction is not an important control on channel change than it can be expected that there is no preference towards any particular direction. If flow direction does indeed factor into controlling patterns of channel change then specific bands of flow direction change would be associated with channel change. For example, if topographic steering (e.g. Dietrich and Whiting, 1991) controls channel change, then it would be expected that deposition and erosion would be associated with bands of minor changes in flow direction (e.g. +/-30 degrees). It is also possible that eddying could control channel change and in this case it would be expected that channel change would be associated with a succession of directional bands ranging from 0 to 360 degrees. Lastly, it is also important to determine if the associations of flow direction and channel change among all 3D histograms are discharge dependent or remain constant. To present the data, only the unsigned data is shown because this level of analysis does not seek to understand whether change occurred on river right or river left. To further simplify presentation of the data, only three bins were selected: 0-30 for straight flow, 30-90 for flow that may be converging, diverging, or beginning to eddy, and 90-360 for flow that has eddying. This is a simplified classification and a more complete method of characterizing the flow structure would entail a complimentary geospatial analysis, but that was beyond the scope of evaluating the effect of topographic steering on channel change.

4.5.3 Autocorrelation of flow width series

Autocorrelation is the cross correlation of data values within a signal with values in the same signal but at specified lag intervals and is a basic tool for determining spatial scales of correlation. Autocorrelation was performed for each flow width series to characterize stage dependent variability of the boundary topography and also to analyze how it changed with increasing discharge. There are multiple variants used to estimate autocorrelation and Cox (1983) provides guidance on the selection of an appropriate function for geomorphic inquiry. An unbiased estimate of autocorrelation for k lags is given by:

$$R_k = \frac{\frac{1}{\mathrm{n-k}}\sum_{\mathrm{i=1}}^{\mathrm{n-k}}(x_i-\bar{x})(x_{i+k}-\bar{x})}{\frac{1}{\mathrm{n}}\sum_{\mathrm{i=1}}^{\mathrm{n-k}}(x_i-\bar{x})^2} \quad (1)$$

where the terms $\frac{1}{\mathrm{n-k}}$ and $\frac{1}{\mathrm{n}}$ account for sample bias (Cox, 1983; Shumway and Stoffer, 2006). Statistical significance was assessed relative to white and red noise autocorrelations, where the latter is essential a first order Markov process (Torrence and Compo, 1998; Newland,1993). The benefit of this approach is that (i) many fluvial geomorphic spatial series display autoregressive properties (Melton, 1962; Rendell and Alexander, 1979; Knighton, 1983; Madej, 2001) and (ii) it provides further context for interpreting results beyond assuming white noise properties. The 95% confidence limits for white noise are given by $-\frac{1}{n}+/-\frac{2}{\sqrt{n}}$ (Salas et al., 1980). For red noise, a first order autoregressive (AR1) model was fit to the standardized residuals for each spatial series and then averaged giving a final model coefficient. Next, 100 random spatial series (each with the same number of points as the flow width spatial series) were generated, and for each one an AR1 model was produced. The average of all 100 AR1 series was then autocorrelated as an estimate for red noise. The decorrelation distance for each data set was inferred as the lag distance where the autocorrelation was ≤ 0.

5 Results and discussion

5.1 Observed channel change and topographic change detection

Combining field observations, aerial imagery and the TCD analysis it is evident that the primary response of the study site to the gravel injection experiment was deposition, as expected, but there were areas of erosion, too (Fig. 4a). For the upstream area the intermediate TCD analysis for the 2007 baseline data set and immediately after the injection predicted that 4,491 metric tonnes were injected in the river prior to the flood season. A subsequent TCD analysis between the January and October, 2011 topographic data sets predicted 111 and 2,245 metric tonnes of deposition and erosion, respectively, confirming that at least 50% of the injected sediments were exported downstream. Performing a similar TCD analysis of the upstream area for the 2007 baseline to when the river was resurveyed in October, 2011 predicted 2,996 and 18 metric tonnes of deposition and erosion, respectively. This implied that along with material export some existing bed material such as large boulders may have shifted during the flood events. In the downstream area for the 2007 to October, 2011 period the TCD analysis predicted 4,039 and 782 metric tonnes of deposition and erosion, respectively. These analyses suggest that of the 4,491 metric tonnes introduced into the river, 80% of it was transported downstream, while the upstream deposition was a combination of existing bed materials being reworked as well as storage of some of the injected sediments. Although not shown here for brevity, histograms of erosion and deposition illustrated that both deposition and erosion occurred primarily in the 0-0.5 m range.

Direct observation and blimp aerial imagery complimented TCD analysis and provided qualitative evidence for the mechanisms of channel change proposed in Table 1 that occurred between January and October 2011. First, particle trapping occurred widespread in interstitial zones within existing bed roughness elements such as boulders, shot rock, and bedrock (Fig. 4b). These areas were not detectable by the TCD analysis but were captured via the aerial photography and field observations (blue outline in Fig. 4a). Second, topographic steering occurred on the upstream face of the cobble bar at station 750 and just upstream of the large boulder at station 590 as well as throughout the downstream section (Fig. 4c). Flow convergence likely occurred at the riffle-pool couplet near stations 150-200, as the downstream pool scoured and the riffle aggraded. Further, curvature of the channel below station 430 appeared to steer flow and sediment to the outer bend where the sediment was deposited within areas associated with bedrock variability on river left opposite of the large cobble and boulder bar (Fig. 4a). Below several bedrock obstructions it appeared that deposits may have formed from eddying out of the main flow path. Finally, at several locations channel expansions appeared to decrease velocity and cause a general tendency for deposition. Where flow presumably moved straight through these expansions, long bands of deposited material appear to have advected downstream.

Erosion from the baseline state was primarily limited to areas influenced by large bedrock protrusions that promoted local scour by convective acceleration. Many of these were very small areas associated with bedrock outcrops on the outside of the bend downstream of station 600. Further, the depth of erosion at these locations was less than 0.5m, which is commensurate with the size of large angular boulders in the river. This suggests that in these areas erosion occurred at bedrock outcrops where existing coarse sediment and boulders were moved. The largest area of erosion occurred at station 175 at a pool that was constricted by bedrock and a large cobble and boulder bar that was immediately downstream of a riffle (Fig. 4a).

5.2 Geomorphic covariance structures and topographic change

The spatial covariance of Z_i and W_{ij} for the three discharges studied show that the river had a complex geomorphic covariance structure (GCS) of wetted width and detrended bed elevation (Fig. 5) related to topographic features. Before relating the GCS structure to channel change, the change in the GCS with discharge and through space from upstream to downstream are described and the way specific topographic features may cause these changes is discussed. Starting at the upstream limit of the gravel injection at station 920 down to approximately station 750 the GCS responded very little to changes in discharge (i.e. covariance is roughly constant), which is consistent with this river section being the most confined. During low flow the cobble-boulder bar on river left creates a very weak GCS, but the GCS strengthens at bankfull flow and then weakens at the highest flow modeled here, illustrating how topographic features can synchronize dynamically over a range of discharge. Just downstream of this area is a constricted boulder and cobble rapid where covariances are negative regardless of flow, with the highest strength at the low flow. Where the river canyon is constricted by bedrock (e.g., stations 600 to 430) the GCS patterns reflect this, as the spatial patterns change very little with discharge. Just below station 430 where the valley width opens the GCS oscillate in sign as higher bed elevations in wider areas and lower bed elevations in narrower areas produce peaks centered on stations 50, 200, and 350. In general this analysis shows that the covarying patterns of Z_i and W_i are representative of how various topographic features synchronize or not depending on discharge.

Linkages were found to exist between the GCS of channel geometry and the peak centerline velocity at each flow (Fig. 5b,c). At the upstream limit the reach was confined and had many large boulders before transitioning into a pool. The result was that initially velocities were relatively high, but then decayed as flow entered the pool near station 780 (Fig. 5b). At approximately station 650 there was a statistically significant peak in velocity at all discharges analyzed in this study. Comparing this with spatial covariance of Z_i and W_{ij} showed that this was due to a negative covariance of wetted width and detrended bed elevation as this area is topographically high but narrow due to a bedrock outcrop. Another statistically significant peak occurred at approximately stations 200 to 150, a transition from a riffle to a pool, where the peak velocity signal phased downstream with increasing discharge into the main zone of erosion predicted by the TCD analysis. Because deposition occurred at and above the riffle and erosion in the downstream pool, this was interpreted as evidence of flow convergence, whereby the velocity signal phases from the riffle to the pool with discharge, analogous to the phase shift mechanism of riffle-pool sustainability described by Wilkinson et al. (2004). Statistically significant low relative velocities were present but not with the same magnitude as high ones. These exceptional lows occurred in areas that were relative expansions or immediately upstream of hydraulic controls such as stations 225, 375, and 725.The bivariate correlation between combinations of V_{ij}, Z_i and W_{ij} series showed at low flow bed elevation controlled the velocity signal but that this changed with discharge, because flow width became more correlated as discharge increased (Table 3). For example, correlations between Z_i and V_i decrease with discharge, while those between V_i and W_i increase. Next, these concepts are extrapolated to illustrate how Z_i and W_i can be used to infer patterns of channel change.

With a linkage between GCS and topographic features established, this section describes how the GCS controlled channel change after gravel injection. The covariances of discharge-specific wetted width and detrended bed elevation with channel change showed a complex array of zones of statistically significant positive covariances (Fig. 6). In some areas channel change was more closely associated with flow width, while in other areas bed elevation was a stronger control. For example, near station 580 there was a statistically significant peak in the covariance of channel change and W_{ij} at low flow, but this weakened with increasing flow until becoming negative at the flood discharge. This suggests that wetted widths at sediment mobilizing flows did not play a role in this feature. However, inspection of the covariance of Z_i and channel change showed a statistically significant peak in this area suggesting that flow width did not control channel change in this area, but bed elevation was more responsible. In some areas, W_{ij} and Z_i may work together such as stations 50 and 470 where there are statistically significant positive peaks for both detrended bed elevation and wetted width with channel change. For example, the covariance strength increased at the riffle near station 200 as the channel widens with discharge. Moreover, at station 175 there was a constricted pool that was a focused zone of erosion. This area had positive covariances of channel change and flow width up until the flood flow where the sign reversed due to the rapid increase in wetted width between the bankfull and flood flow as the water begins to overtop the adjacent cobble bar. The covariance patterns of wetted width and channel change thus illustrate how varying and complex channel topography can affect erosion and deposition depending on how discharge interacts with these features. Bivariate r values show that there are some interdependent fluctuations in covariances, but the more different the flow is, the more the pattern of co-dependence changes (Table 4). For example, the bivariate correlation between covariances for the low and bankfull flow widths versus channel change was very high, but that between covariances for low and flood flows widths versus channel change was low.

5.3 Flow direction change and topographic change

Some of the emergent deposits shown in the TCD plots were not explained by the covariance analyses, suggesting mechanisms other than flow convergence were responsible. For example, at approximately station 600 there was a gravel bar deposited upstream of a large boulder and regardless of discharge there was not a statistically significant covariance, which suggests that changes in flow width did not control channel change in this location. The final test of topographic controls on channel change showed that flow steering had a strong control on channel change (Fig. 7), as evidenced by the increasingly strong associations of low flow direction change (e.g. <30 degrees) with channel change. Starting at the lowest discharge 84% of channel change was associated with flow directions within +/- 30 degrees and this percentage increased to 97% at the highest discharge modeled. This supports the hypothesis that topographic steering of flow and sediment was a strong control on channel change.

There was, however, a decreasing association of channel change with the change in flow direction in the remaining bins that was related to more complex flow structures such as eddies (Fig. 7). At the low flow of 28.3 m^3/s there was 9% of the total channel change associated with flow direction changes between +/-90 and 360 degrees(Fig. 7a). At the 141.5 m^3/s discharge this percentage dropped to 4%, and at the highest discharge modeled it decreased further to only 1% (Fig. 7c). This further confirms that at the highest discharges topographic steering routed sediment downstream and in some cases into obstructions. To further illustrate this phenomenon, Fig. 8 shows how flow direction changes with increasing discharge over an emergent gravel bar near station 610. At low flow the deposit steers flow directions, at bankfull an eddy is located over it, and at the flood flow the gravel is essentially pushed into the boulder obstruction. Because the sharp rising limb of the flood hydrograph deposited gravel can get pushed into these zones and then effectively cut off from the main downstream path before the flow can fully route the gravel past the boulder. Overall, this flow dependent model is similar to the Rathburn and Wohl (2003) eddy deposit model but for gravel sediments that travel as bedload.

5.4 Autocorrelation of flow widths

The autocorrelation of flow-dependent width series found that as flow increased the spatial scale of correlations also increased (Fig. 9). Further, the flow-dependent autocorrelation illustrates how each flow stage is hierarchically nested within the stage above it. For 28.3 and

141.5 m^3/s flow the series was decorrelated at a distance of 68 m, whereas for of 242.8 m^3/s the series decorrelated at 525 m. At ~ 175 m there were statistically significant correlations in flow width that reverse from being negative at the 28.3 m^3/s and then positive at 141.5 m^3/s. However, at approximately a lag distance of 350 m the magnitude of autocorrelation increased with increasing discharge. Further, the range of lag distances associated with this peak also increased, suggesting that correlations in flow width increase in magnitude and scale with discharge. Comparing these series to the red noise autocorrelation, all positive correlations at lags greater than 300 m were statistically significant. The exclusively positive autocorrelation of flow width at 242.8 m^3/s illustrates the effect of increasing valley width as the river corridor opens up and widens at the downstream end of the study site. Thus, with increasing flow stage channel width becomes increasingly more organized as it begins to follow the valley walls, meaning that wide areas get larger and have the potential to attenuate larger scale depositional features. For the EDR this has been confirmed as at least two large floods of 4,361 m^3/s in 1997 and 2,707 m^3/s in 2005/2006 have deposited large cobbles, angular shotrock, and boulders on the large alluvial bar below station 430 (Pasternack et al., 2010).

5.5 Hydrologic and topographic modulation of process-blending in mountain rivers

The complex behaviors reported in this study demonstrate that flow hydrology modulates the activation of topographic features that control channel change in mountain rivers through a diverse array of channel change mechanisms such as topographic steering, particle trapping, flow convergence, eddying, and backwatering. The significance of this finding is that no single process controlled channel change; a continuum of hydrodynamic and sediment transport mechanisms are responsible as modulated by the interaction of flow hydrology and boundary topography. While each of the mechanisms described earlier were partially responsible for the observed channel change, some were more prevalent in specific areas. Selective deposition of sediments through particle trapping in interstitial zones of existing bedrock and boulder substrate occurred widespread. Topographic steering into boulder and bedrock obstructions as well as topographic high points occurred in at least two areas, the main channel before the rapid and the face of the cobble-boulder bar at station 720 and the large boulder at station 580. Just below the large boulder from station 570 to 530 sediments eddied out behind the obstruction. In addition to these smaller scale mechanisms, from station 430 down to the study limit changes in flow width (flow convergence) and curvature (topographic steering) were important controls on the patterns of channel change observed. For example, the riffle-pool unit at stations 150-200 had a downstream phase shift of the velocity signal from the low to high discharge from the riffle to the pool (Wilkinson et al., 2004). There was also a corresponding shift in the magnitude and sign of the GCS of flow width and channel change. This suggests that flow convergence in the pool at the higher discharges mediated pool scour and as well as the accumulation of material at the upstream riffle from reduced velocities. Finally at the downstream limit deposition was spread amongst the channel bed as the river widens even more. Overall, each channel change mechanism proposed occurred through the study reach depending on the type of boundary topography and whether the flow stage activated it.

Fig. 10 is a conceptualization of the interplay between flow stage and the variable topography representative of complex mountain river channels that predominantly transport gravel and cobble sediments. At the lowest discharge, when perhaps only smaller fractions of gravel are in transport, flow is steered around emergent gravel deposits, a large boulder, and bedrock walls. At the crests of the two riffles there would be flow convergence and this would also generate an upstream backwater in the pool, so that any material transported from the riffles would be attenuated in the pools. When the discharge is increased to where the upper two (and smaller) emergent bars are inundated, flow is steered into the boulder and converges into the adjacent pool, while downstream a recirculating eddy would form. This would lead to increased bedload transport at the riffles and subsequent gravel deposits forming at the head of the boulder as well as any material routed through the boulder pool being pulled into the downstream eddy. Upstream of the boulder, the constriction would cause a backwater that may further reduce material transport, inducing upstream deposition. Given an even higher discharge, the boulder would still be inundated and the lower gravel bar is partially inundated so that flow would primarily be steered by the lower cobble bar and valley walls. At this stage the zones of flow convergence would shift to the partially constricted pool, where transported sediments would deposit on the next downstream riffle. Further, the inundated boulder would continue to attenuate sediments that are steered into it, enhancing the depositional form at the previous flow stage. Thus, this conceptualization demonstrates that depending on the flow stage, different topographic features can induce a suite of hydrodynamic mechanisms that can modulate channel change. Finally, the duration of each flow magnitude would further reinforce how relevant particular topographic features are in mediating channel change.

5.6 Broader implications

The results of this study are relevant in at least four applications in river management and rehabilitation. First, in developed nations many mountain rivers experience some form of flow regulation from competing demands, such as whitewater recreation, sensitive aquatic species, and water supply for agriculture. However, the joint relationship between hydrologic and topographic variability needed to maintain these environments is often not considered. In this study it was shown that topographic features of all spatial scales are important in controlling the spatial patterns of channel change. In regulated systems that do not account for the activation of multiple scales of topography in forming and maintaining diverse spatial habitat units there may be a risk of oversimplifying the physical template of these types of rivers. Moreover, river restoration could benefit from this study in that both hydrologic variability and boundary topography need to be considered jointly in reinstating fluvial processes that create and form habitat. Second, spatial covariance patterns of channel geometry may be able to predict the location and relative magnitude of channel change from river rehabilitation actions, such as gravel augmentation. In this study, regardless of discharge or stage, areas of relatively high channel width were associated with the most deposition of injected gravels. Therefore, it may be possible to detect channel change by simply analyzing spatial patterns of channel width and bed elevation from detrended topography. Further, this study has shown topographic series are a valuable input to statistical analysis that can be used to infer processes in rivers generally and help in predicting their response to changes in sediment supply. These tools may play a valuable role in detecting geomorphic processes as remotely sensed data collection continues to grow. Finally, as many topographic aspects of mountain rivers are fixed in the engineering sense (e.g. bedrock and large boulders), it is thought that flow, sediment, and woody material augmentation are the primary tools in managing and rehabilitating these types of environments.

5.7 Study limitations and future work

There are some limitations to this study that deserve attention. Hydrologic variability was assessed relative to the interaction of flow magnitude and topography that occurred within the flood season, and not with flow duration, because of the temporal resolution of the TCD analysis. Flow duration and hydrograph shape are likely important in assessing channel change, but it remains difficult to assess mountain rivers at finer temporal windows because flows do not always recede enough for data to be collected safely. Further, as it is often stated correlation does not always imply causation, but this study utilized an extensive suite of modern fluvial geomorphic tools that give significant mechanistic interpretation to the statistical analyses performed herein. Moreover, model direction evaluation was performed at baseflow, bankfull, and flood discharges. Thus, this study assumes that model performance evaluated at lower discharges may be valid at higher discharges. To date, there are no safe or feasible methods of evaluating flow directions during floods in mountain rivers, but there are also no fundamental differences in the physics of water flow either that would suggest a difference in performance. Barker (2011) and Pasternack and Senter (2011) both assessed 2D models over a wide range of flows and found no flow-dependent differences in model performance. Further, while this study used a very well validated 2D model it could also be that 3D important mechanisms may be more responsible, especially at flood flows where bedrock features become submerged. Future research should explore how important 3D hydrodynamics are in influencing flow direction and channel change. These points notwithstanding the validation data presented here represent state of the science capabilities and some of the best reported data observations in the peer-reviewed literature.

6 Conclusions

This study used a diverse array of fluvial geomorphic tools such as high resolution bathymetric and topographic mapping, 2D modeling, topographic change detection, kite-blimp aerial photography, and geomorphic covariance analyses coupled with traditional field based observations to analyze controls on channel change in a mountain river. While the experiment took place in a large, regulated mountain river it was relatively controlled in that none of the injected gravel or cobble size fractions were present in the reach prior to the injection. Flood flows after the injection and the lack of existing mobile bed material led deposition to be the major response of the river to the injection. Prior studies undeniably suggested the channel change mechanisms investigated herein, but this study fills a crucial gap between detailed field studies at smaller spatial scales and observation driven studies at larger spatial scales. A variety of mechanisms of channel change were qualitatively and quantitatively confirmed to effect channel change including particle trapping, eddying, topographic steering, and flow convergence. Perhaps most importantly, no single mechanism explained all of the observed patterns of channel change. Rather, it is thought that process-blending of multiple mechanisms, as modulated by flow hydrology, controls channel change in mountain rivers through the dynamic activation of complex river corridor topography.

Acknowledgements

Financial support was provided by a Henry A. Jastro Graduate Research Award and a research grant from the U. S. Army Corps of Engineers (award # W912HZ-11-2-0038). The baseline topographic map for 2007 was prepared by Hamish Moir, Jason White, Aaron Fulton, Scott

Morford, and Environmental Data Solutions. The 2010-2011 data collection campaign had field support provided by Lloyd Howry of the Army Corps of Engineers. Rusty Barker assisted in developing initial Excel© programming used to determine Cartesian quadrants for flow vectors. This manuscript greatly benefited by reviews by Andrew Gray, Matthew Vaughan, and an anonymous reviewer.

References

Barker, J.R., 2011. Rapid, abundant velocity observation to validate million-element 2D hydrodynamic models. M.S. Thesis, University of California at Davis, Davis, CA.

Blanckaert, K., 2010. Topographic steering, flow recirculation, velocity redistribution, and bed topography in sharp meander bends, Water Resour. Res., 46, W09506, pp. 23.

Brayshaw, A. C., 1985. Bed microtopography and entrainment thresholds in gravel-bed rivers. Geological Society of America Bulletin 96.

Brown, R. A., and Pasternack, G. B., 2008. Engineered channel controls limiting spawning habitat rehabilitation success on regulated gravel-bed rivers. Geomorphology 97.

Brown, R.A. and Pasternack, G.B., 2012. Monitoring And Assessment Of The 2010-2011 Gravel/Cobble Augmentation In The Englebright Dam Reach Of The Lower Yuba River, CA. University of California Technical Report, Davis, CA.

Buffington, J. M., Lisle, T. E., Woodsmith, R. D., Hilton, S., 2002. Controls on the size and occurrence of pools in coarse-grained forest rivers. River Research and Applications 18.

Carbonneau, P., Fonstad, M., Marcus, W., Dugdale, S., 2012. Making riverscapes real. Geomorphology 137.

Carley, J. K., G. B. Pasternack, J. R. Wyrick, J. R. Barker, P. M. Bratovich, D. A. Massa, G. D. Reedy, Johnson,T.R., 2012. Significant decadal channel change 58–67years post-dam accounting for uncertainty in topographic change detection between contour maps and point cloud models. Geomorphology 179.

Cenderelli, D. A., Cluer, B.L., 2013. Depositional Processes and Sediment Supply in Resistant-Boundary Channels: Examples from Two Case Studies. In: Tinkler, T.J., Wohl, E.E., (Eds.). Rivers Over Rock: Fluvial Processes in Bedrock Channels, American Geophysical Union, Washington, D. C.

Cox, N. J., 1983. On the estimation of spatial autocorrelation in geomorphology. Earth Surf. Process. Landforms 8, 89–93.

Fonstad, M. A., Marcus, W.A., 2010. High resolution, basin extent observations and implications for understanding river form and process. Earth Surface Processes and Landforms 35.

Fryirs, K., Brierley, G., 2010. Antecedent controls on river character and behaviour in partly confined valley settings: Upper Hunter catchment, NSW, Australia, Geomorphology 117.

Grant, G. E., Swanson, F. J. Wolman, M. G., 1990. Pattern and origin of stepped-bed morphology in high-gradient streams, Western Cascades, Oregon. Geological Society of America Bulletin 102.

Grant, G., Swanson, F., 1995. Morphology and processes of valley floors in mountain streams, western Cascades, Oregon. In: Costa, J.E., Miller, A.J., Potter, K.W., Wilcock, P.R (Eds.), Natural and Anthropogenic Influences in Fluvial Geomorphology: the Wolman Volume. Geophysical Monograph No. 89. American Geophysical Union. Washington, D.C.

Harrison, L. R., Keller, E.A., 2007. Modeling forced pool–riffle hydraulics in a boulder-bed stream, southern California. Geomorphology 83.

Howard, A., Dolan, R., 1981. Geomorphology of the Colorado River in the Grand Canyon. The Journal of Geology 89.

Hynes, H. B., 1970. The ecology of running waters. University of Toronto Press.

Knighton, A., 1983. Models of stream bed topography at the reach scale. Journal of Hydrology 60.

Legleiter, C., Phelps, T., Wohl, E.E., 2007. Geostatistical analysis of the effects of stage and roughness on reach-scale spatial patterns of velocity and turbulence intensity. Geomorphology 83.

Lisle, T., 1986. Stabilization of a gravel channel by large streamside obstructions and bedrock bends, Jacoby Creek, northwestern California. Geological Society of America 97.

MacVicar, B. J., Roy, A.G., 2007. Hydrodynamics of a forced riffle pool in a gravel bed river: 2. Scale and structure of coherent turbulent events. Water Resources Research 43.

MacWilliams, M. L., Wheaton, J. M., Pasternack, G. B., Street, R. L., Kitanidis, P.K., 2006. Flow convergence routing hypothesis for pool-riffle maintenance in alluvial rivers. Water Resources Research 42.

Madej, M. A., 2001. Development of channel organization and roughness following sediment pulses in single-thread, gravel bed rivers. Water Resources Research 37.

Melton, M. A., 1962. Methods for measuring the effect of environmental factors on channel properties. Journal of Geophysical Research 67.

Merwade, V. M., Maidment, D. R., Goff, J.A., 2006. Anisotropic considerations while interpolating river channel bathymetry. Journal of Hydrology 331.

Milan, D., Heritage, G., Large, A., Fuller, I. 2011. Filtering spatial error from DEMs: Implications for morphological change estimation, Geomorphology 125.

Montgomery, D.R., Buffington, J.M., 1997. Channel-reach morphology in mountain drainage basins. Geological Society of America Bulletin 109, 596-611.

Montgomery, D.R., Collins, B.D., Buffington, J.M., Abbe, T.B., 2003. Geomorphic effects of wood in rivers. In: Gregory, S. V. Boyer, K.L., Gurnell, A.M. (Eds.) The ecology and management of wood in world rivers. American Fisheries Society Symposium 37.

Newland, D.E., 1993. An introduction to random vibrations, spectral & wavelet analysis. Dover Publications. New York, New York.

O'Connor, J. E., Webb, R. H., Baker, V. R., 1986. Paleohydrology of pool-and-riffle pattern development: Boulder Creek, Utah. Geological Society of America Bulletin 97.

Pasternack, G.B., 2011. 2D Modeling and Ecohydraulic Analysis. Createspace: Seattle, WA.158 pp.

Pasternack, G. B., Fulton, A. A., Morford, S. L., 2010. Yuba River analysis aims to aid spring-run Chinook salmon habitat rehabilitation. California Agriculture 64.

Pasternack, G. B., Senter, A.E. 2011. 21st Century instream flow assessment framework for mountain streams. California Energy Commission, Public Interest Energy Research, CEC-500-2013-059, Sacramento, CA.

Rathburn, S., Wohl, E., 2003. Predicting fine sediment dynamics along a pool-riffle mountain channel. Geomorphology 55.

Rendell, H., Alexander, D., 1979. Note on some spatial and temporal variations in ephemeral channel form. Geological Society of America Bulletin 90.

rocko 12/25/2013 2:05 PM
Deleted: ,

Salas, J. D., Delleur, J. W., Yevjevich, V. Lane, W. L., 1980. Applied Modeling of Hydrologic Time Series. Water Resources Publications. Littleton, Colorado.

Sawyer, A. M., Pasternack, G. B., Moir, H. J., Fulton, A. A., 2010. Riffle-pool maintenance and flow convergence routing confirmed on a large gravel bed river. Geomorphology 114.

Smith, J. D., Mclean, S.R., 1984. A model for flow in meandering streams. Water Resources Research 20.

Thompson, D.M., 2007. The characteristics of turbulence in a shear zone downstream of a channel constriction in a coarse-grained forced pool. Geomorphology 83.

Thompson, D. M., Wohl, E.E.,2009. The linkage between velocity patterns and sediment entrainment in a forced-pool and riffle unit. Earth Surface Processes and Landforms 34.

Thompson, D.M., 2011. The velocity-reversal hypothesis revisited. Progress in Physical Geography 35.

Torrence, C., Compo, G., 1998. A practical guide to wavelet analysis. Bulletin of the American Meteorological Society 79.

Wheaton, J. M., Brasington, J., Darby, S.E., Merz, J., Pasternack, G.B., Sear,D., Vericat, D., 2010. Linking geomorphic changes to salmonid habitat at a scale relevant to fish. River Research and Applications, 26.

Wheaton, J. M., Brasington, J., Darby, S.E., Sear, D.A., 2009. Accounting for uncertainty in DEMs from repeat topographic surveys: improved sediment budgets. Earth Surface Processes and Landforms 35.

White, J. Q., Pasternack, G. B., Moir, H.J., 2010. Valley width variation influences riffle–pool location and persistence on a rapidly incising gravel-bed river. Geomorphology, 121.

Whiting, P. J., Dietrich, W.E., 1991. Convective accelerations and boundary shear stress over a Channel Bar. Water Resources Research 27.

Wilkinson, S. N., Keller, R. J., Rutherfurd, I. D. 2004. Phase-shifts in shear stress as an explanation for the maintenance of pool–riffle sequences. Earth Surface Processes and Landforms 29.

Wohl, E.E. 2000. Mountain Rivers. Water Resources Monograph 14. American Geophysical Union.Washington, D.C.

Wohl, E., Kuzma, J. N., Brown, N.E., 2004. Reach-scale channel geometry of a mountain river. Earth Surface Processes and Landforms 29.

Wohl, E.E., Merritt, D.M., 2001. Bedrock channel morphology. Geological Society of America Bulletin 113, 1205-1212

Wohl, E., and Legleiter, C., 2003. Controls on Pool Characteristics along a Resistant-Boundary Channel. Journal of Geology 111.

Woodsmith, R., Hassan, M. 2005. Maintenance of an obstruction-forced pool in a gravel-bed channel: streamflow, channel morphology, and sediment transport, In: Garcia, Celso and Batalla, Ramon J., (Eds.) Developments in Earth Surface Processes,vol.7. Elsevier.

Wyrick, J. Pasternack, G.B., 2012. Landforms of The Lower Yuba River. Prepared for The Lower Yuba River Accord Planning Team. University of California, Davis.

List of Tables

Name	Channel Change Mechanisms	Scale (Channel Widths)	Dominant Topographic Elements*	Approximate Ranges of Daily Flow Exceedance **	References
Particle trapping	Selective deposition can occur as bedload in motion will get trapped upstream of existing bed material larger than that in transport or within interstitial pockets.	$<10^{-1}$	Cobbles, bedrock outcrops, boulders	Limiting flow based on incipient particle motion and can occur at all flows greater than this	Brayshaw, 1985; Grant et al., 1990
Topographic steering	Topographic steering can push material intransport into obstructions or other non-mobile depositional forms. Steering can also follow the curvature of broader scale landforms inducing deposition or erosion due to	10^{-1} - $>10^{1}$	Gravel/cobble bars, bedrock outcrops, boulders, debris jams, bedforms	Topographic steering can occur at all flows so long as the boundary is immobile	Lisle, 1986; Whiting and Dietrich, 1991; MacWilliams et al., 2006; Thompson, 2007; Thompson et al., 2009; Blanckaert , 2012;
Flow convergence	Vertical and lateral funneling of flow momentum as mediated by variations in the width of boundary topography. As a dual stage process, peak velocity at low flow over the riffle will phase downstream into the pool at high flow.	10^{0}->10^{1}	Gravel/cobble bars, bedrock outcrops, debris jams, bedforms	10 - 50%	MacWilliams et al., 2006; Harrison and Keller, 2007; Thompson et al., 2009; Sawyer et al., 2010
Eddying	Immediately downstream of obstructions abrupt expansion eddies may form and material can get pushed and pulled into the recirculation zone and deposit.	10^{-1}-10^{0}	Large bedrock outcrops (~1/3 bankfull width), multiple boulders, bedforms	> 50-67%	Lisle, 1986; Thompson et al., 1999; Rathburn and Wohl, 2003; Thompson, 2007; Thompson et al., 2009
Backwatering	Valley scale changes in width can modulate broader scale decreases in flow competence from backwater effects that lead to deposition.	$>10^{1}$	Valley scale changes in width, bedrock, large cobble/boulder bars, debris jams, bedforms	< 10%	O'Connor et al., 1986; Jaeggi , 1987; Howard and Dolan, 1981; Cenderelli and Cluer, 1998

* Does not include anthropogenic features

**Assumed for rivers in the Northwestern United States

Question	**Test**	**Hypothesis**	**Channel change mechanism (s) evaluated**
Is there a covarying pattern of flow width and bed elevation and how does this change with discharge?	GCS* of flow width and bed elevation	There will be statistically significant patterns of covarying flow width and bed elevation associated with	flow convergence
When and where does flow width and/or bed elevation control velocity?	GCS of flow width and velocity and bed elevation and velocity	The strength of velocity correlations will be highest for bed elevation at the lower discharge and highest for flow width at the highest discharge.	
When and where does flow width and/or bed elevation control channel change?	GCS of flow width and channel change and thalweg bed elevation and channel change	Channel change will correlate with areas of both increased flow width and thalweg bed elevation depending on the type of landform.	topographic steering, flow convergence
Does flow direction control channel change and how does that change with discharge?	Histograms of channel and flow direction change	Channel change will primarily be associated with the main flow direction of the channel and this will be greatest at the highest discharge modeled.	topographic steering, flow convergence, eddying
Does flow direction control channel change and how does that change with discharge?	Autocorrelation of flow widths	Width series will become more correlated with increasing discharge	topographic steering, valley scale backwater

* A geomorphic covariance structure (GCS) is a bivariate serial correlation

		Relative velocity		
		28.3 m3/s	141.5 m3/s	242.8 m3/s
	Detrended bed elevation	**0.55**	**0.40**	0.15
	28.3 m3/s	**-0.60**	**-0.62**	**-0.56**
Relative flow width	141.5 m3/s	**-0.49**	**-0.69**	**-0.71**
	242.8 m3/s	**-0.47**	**-0.67**	**-0.81**

Covariance	C(Z,W141.5)	C(Z,W242.8)	C(Z,CC*)	C(W28.3,CC)	C(W141.5,CC)	C(W242.8, CC)
C(Z,W28.3)	**0.76**	**0.48**	0.06	0.14	0.18	0.17
C(Z,W141.5)		**0.79**	-0.11	0.18	0.13	0.13
C(Z,W242.8)			-0.10	0.23	0.15	0.00
C(Z,CC)				**-0.32**	-0.14	-0.06
C(W28.3,CC)					**0.80**	**0.41**
C(W141.5,CC)						**0.72**

*CC ~ channel change

Table 1. Channel change mechanisms investigated in this study along with approximate spatial scales of causative topographic features, approximate ranges of flow frequency they occur at, and sources from the literature.

Table 2. Channel change mechanisms and alternative hypotheses for each study test.

Table 3. Pearson's correlation coefficient (r) between detrended bed elevation, velocity and width for 28.3, 141.5, and 282.4 m3/s to determine if they are interdependent. Bold values are statistical significant at the 95% level.

Table 4. Pearson's correlation coefficient (r) between various covariances of detrended bed elevation, flow width and channel change for 28.3, 141.5, and 282.4 m3/s to determine if they are interdependent. Bold values are statistical significant at the 95% level.

List of Figures

Fig. 1. Aerial photograph of study area (A). The blue lines delineate the upstream and downstream limits of the study while the red line delineates the upstream and downstream topographic change scenarios. The white arrows show the location and orientation of photographs (B,C). Flow shown in both the air photo was ~28.3 m^3/s.

Fig. 2. Hydrograph following the gravel injection in January, 2011 up to the October, 2011 surveys.

Fig. 3. Conceptual key for flow direction change analysis. Assuming flow is downstream negative values correspond to flow direction changes in which a flow vector is oriented towards river right and positive values when a flow vector is oriented towards river left. Similarly, negative and positive values greater than 90 degrees correspond to flow vectors that are at the onset of eddying upstream.

Fig. 4. Map of topographic change (A) for the 2007-October, 2011 epoch overlain on the blimp imagery. The blue outline delineates sediment deposits detected through ground observations and visible in the image, but not detected from the TCD analysis. An example of sediment deposits that were undetected in the TCD analysis due to interstitial void filling and topographic steering behind existing cobble clusters is shown in (B), taken on the cobble and boulder bar on river left at station 700. The largest visible emergent deposit is shown in (C) where material was topographically steered into the face of the large boulder at station 580. Flow shown in both the air photo and images was ~28.3 m^3/s.

Fig. 5. Map of detrended topography and flow widths (A) where the color darkness of the blue lines represent inundation extents for 28.3, 141.5, and 242.8 m^3/s. Geomorphic covariance structure (GCS) of centerline detrended bed elevation and flow width for 28.3, 141.5, and 242.8 m^3/s (B) and the standardized velocity signal (C) for the same three flows. Grey lines on (B) and

(C) represent one standard deviation. Together these plots illustrate the relationship between topographic features and flow-dependent changes in the GCS and velocity.

Fig. 6. GCS of channel change with the three flows modeled (A) and with centerline detrended bed elevation (B) illustrating which areas of channel change are positively associated with changes in flow width and bed elevation.

Fig. 7. The 3D histogram of channel change and flow direction change for (A) 28.3 m^3/s, (B) 141.5 m^3/s, and (C) 242.8 m^3/s.

Fig. 8. 2D model derived flow vectors overlaid on a cm scale resolution air photograph (A) 28.3 m^3/s, (B) 141.5 m^3/s , and (C) 242.8 m^3/s. Blue lines correspond to the 2D model predicted inundation extent for each discharge. Flow shown in aerial images was ~28.3 m^3/s.

Fig. 9. Autocorrelation of flow width for the three discharges modeled along with theoretical red and white noise processes. The broadening of correlated length scales illustrates that with increasing discharge larger scale topographic features become activated.

Fig. 10. Conceptualization of the interplay between flow stage and topographic variability and channel change mechanisms. The gray colors represent different relative heights of topographic features with darker colors corresponding to higher elevations. The blue shading represents the inundation extent. As flow stage increases flow patterns are steered by different topographic features which in turn control the channel change mechanisms described in the text.

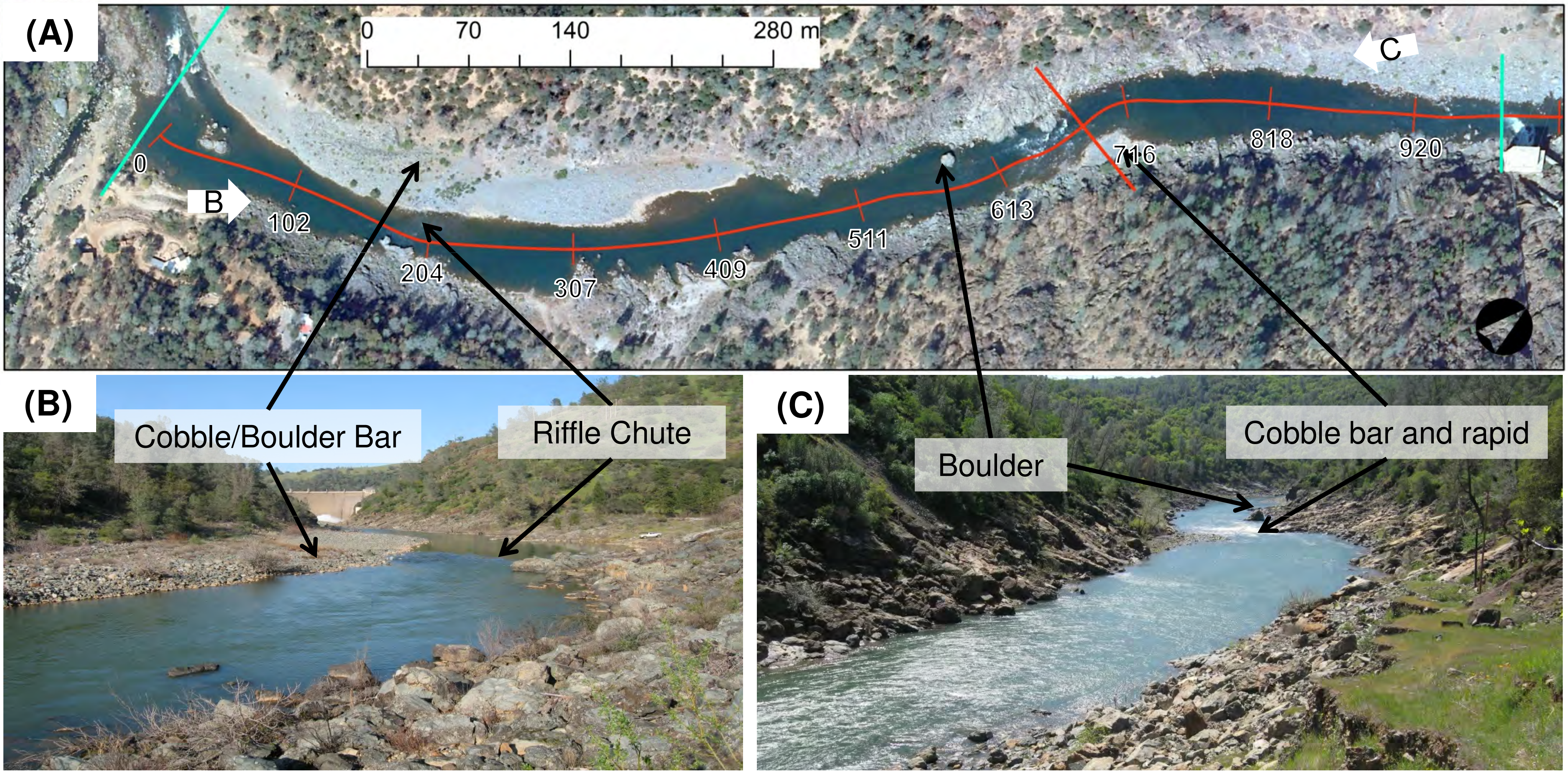

(A)
0
70
140
280 m
C
B
0
102
204
307
409
511
613
716
818
920
(B)
Cobble/Boulder Bar
Riffle Chute
(C)
Boulder
Cobble bar and rapid

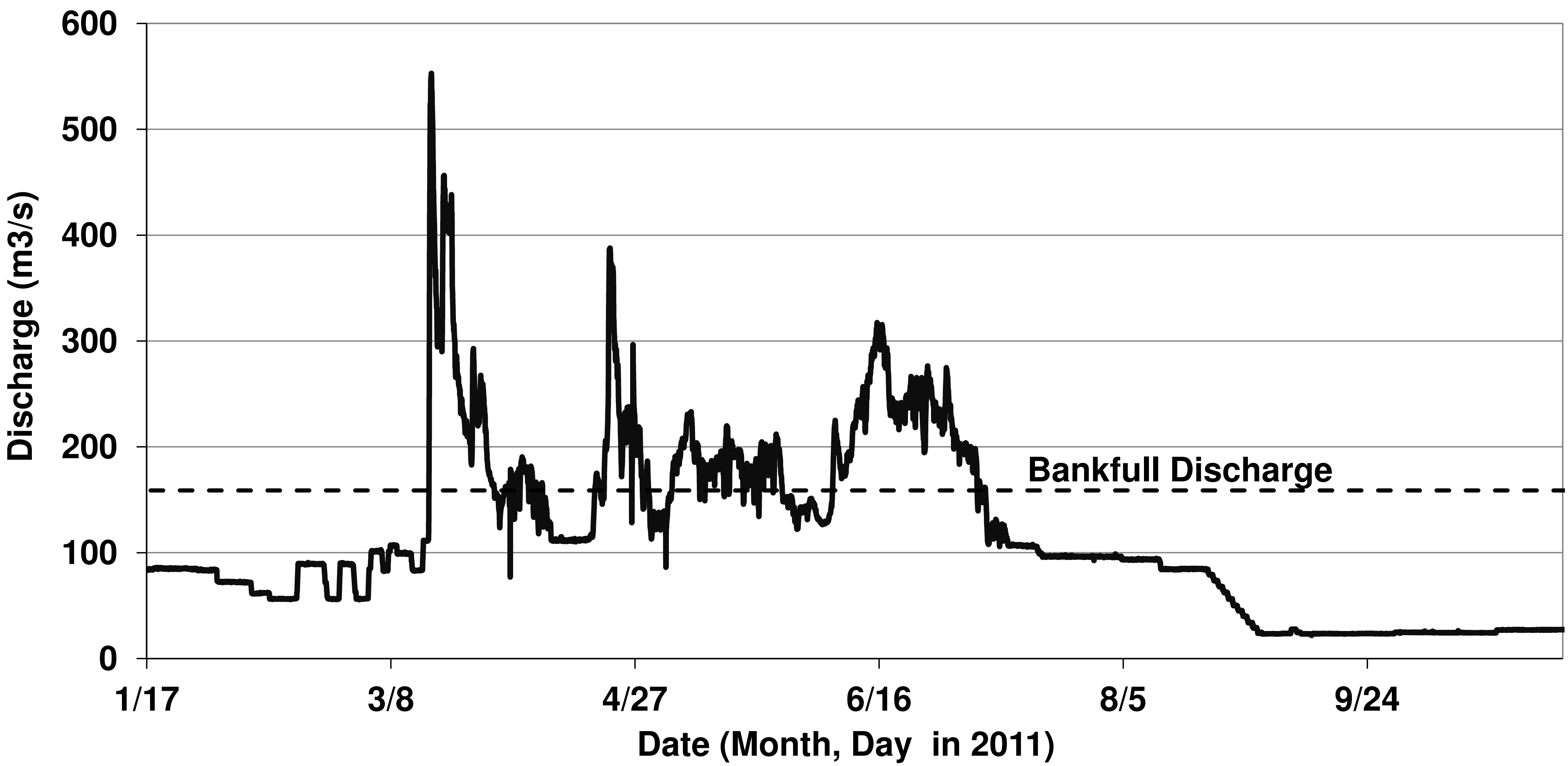
600
500
400
300
200
100
0
Discharge (m3/s)
Bankfull Discharge
1/17
3/8
4/27
6/16
8/5
9/24
Date (Month, Day in 2011)

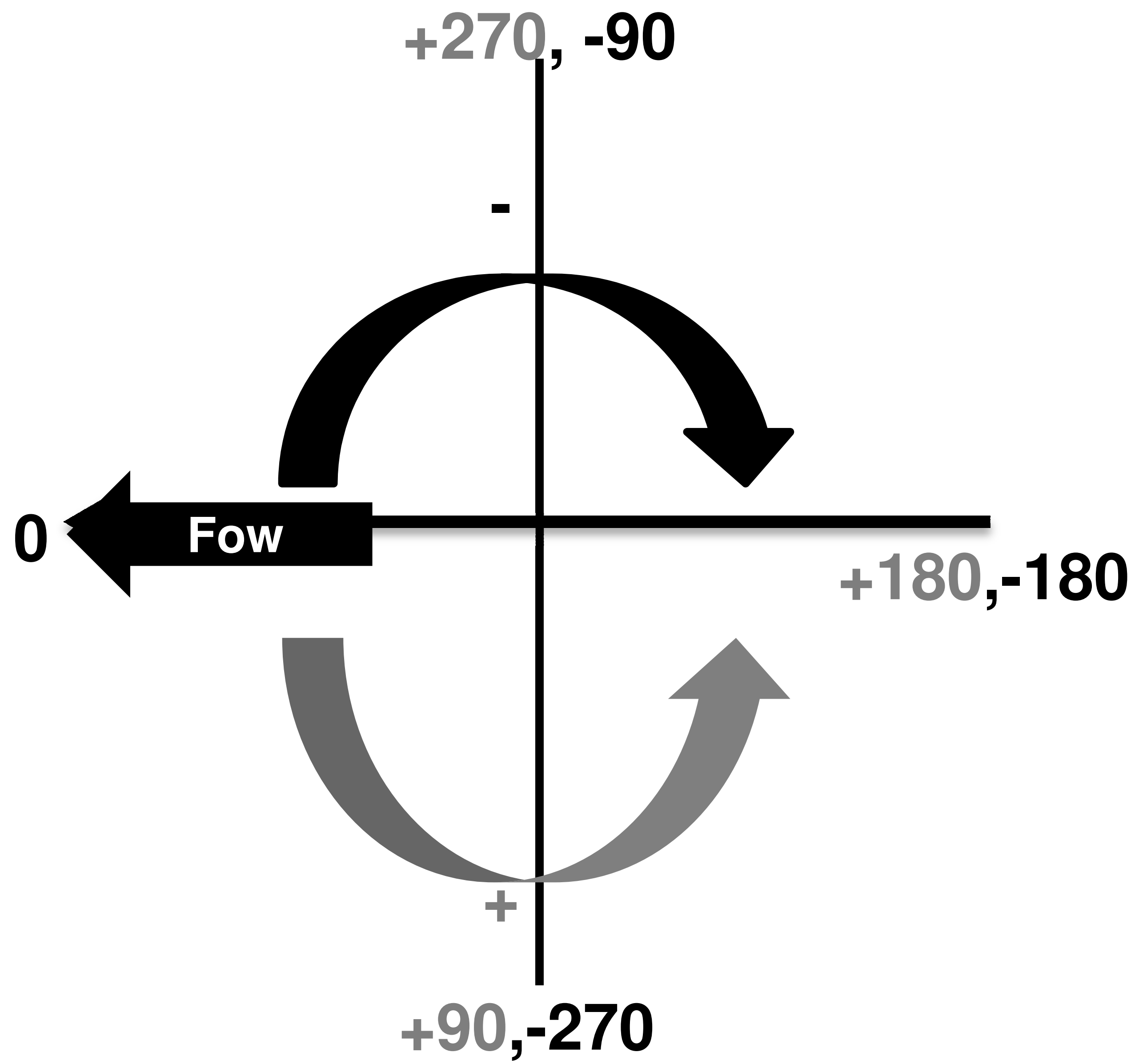

$$\Delta direction = \Phi_{point} - \Phi_{centerline}$$

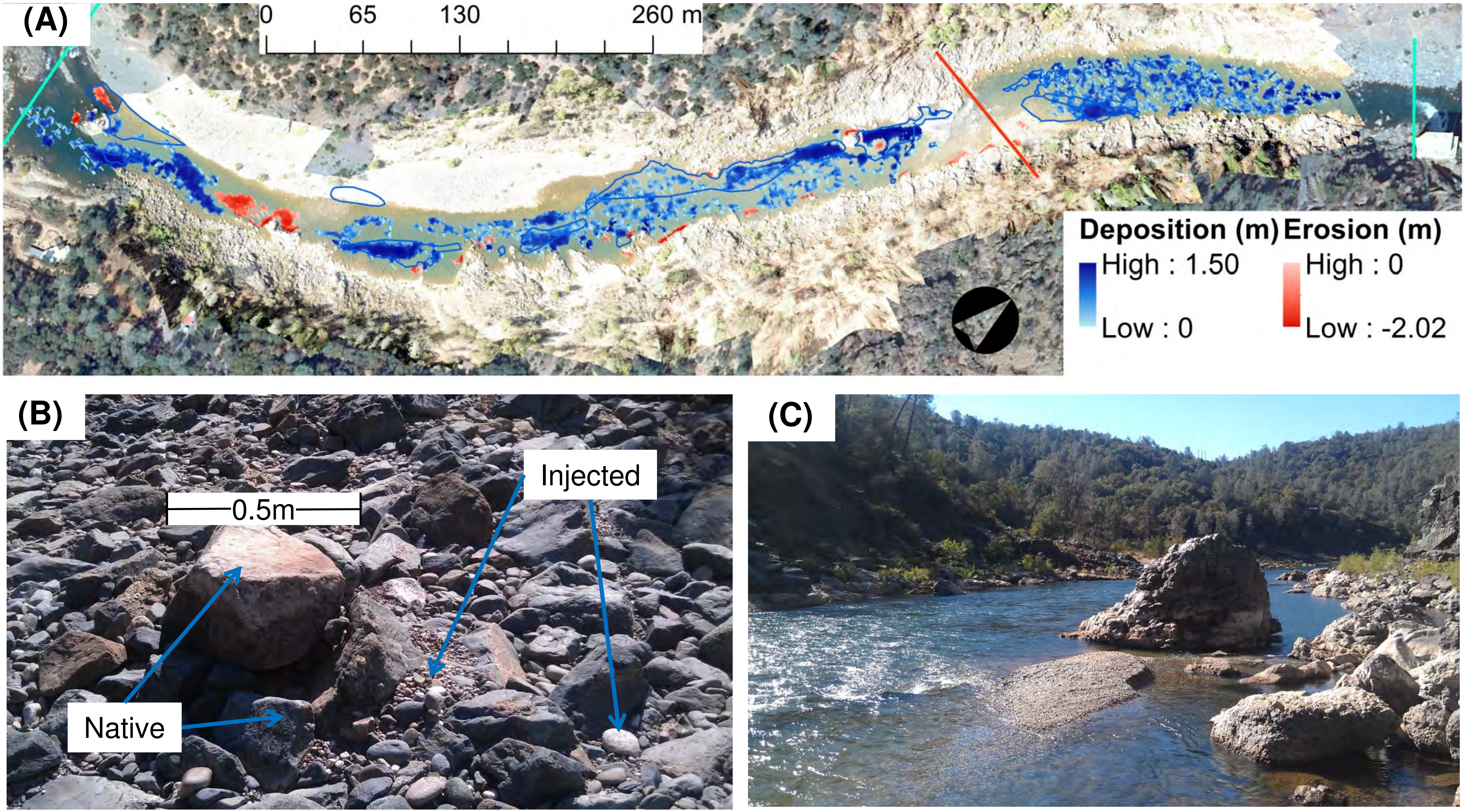
(A)
0
65
130
260 m
Deposition (m)
High : 1.50
Low : 0
Erosion (m)
High : 0
Low : -2.02
(B)
0.5m
Injected
Native
(C)

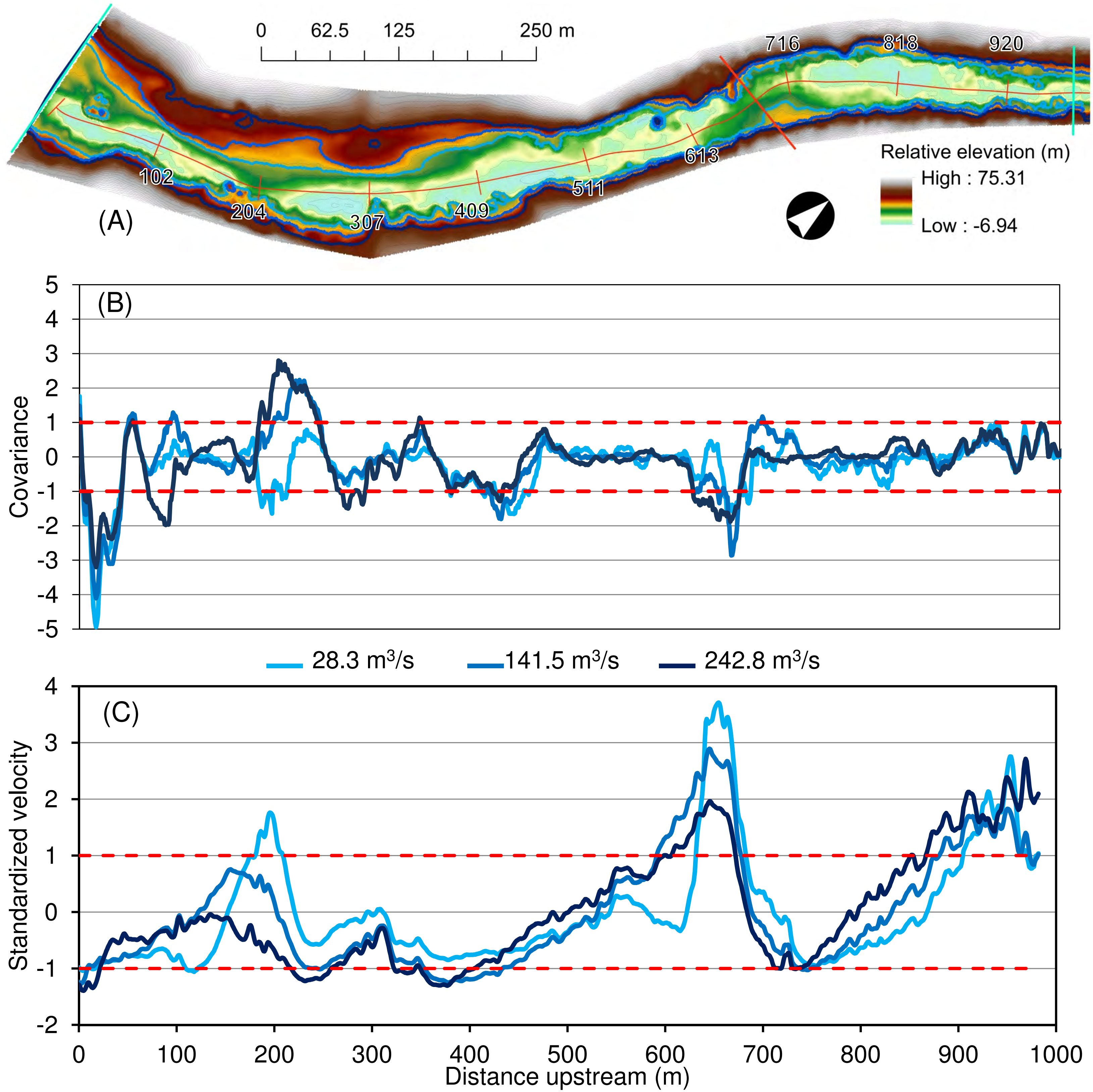

0
62.5
125
250 m
102
204
307
409
511
613
716
818
920
(A)
Relative elevation (m)
High : 75.31
Low : -6.94
(B)
Covariance
5
4
3
2
1
0
-1
-2
-3
-4
-5
28.3 m³/s
141.5 m³/s
242.8 m³/s
(C)
Standardized velocity
4
3
2
1
0
-1
-2
0
100
200
300
400
500
600
700
800
900
1000
Distance upstream (m)

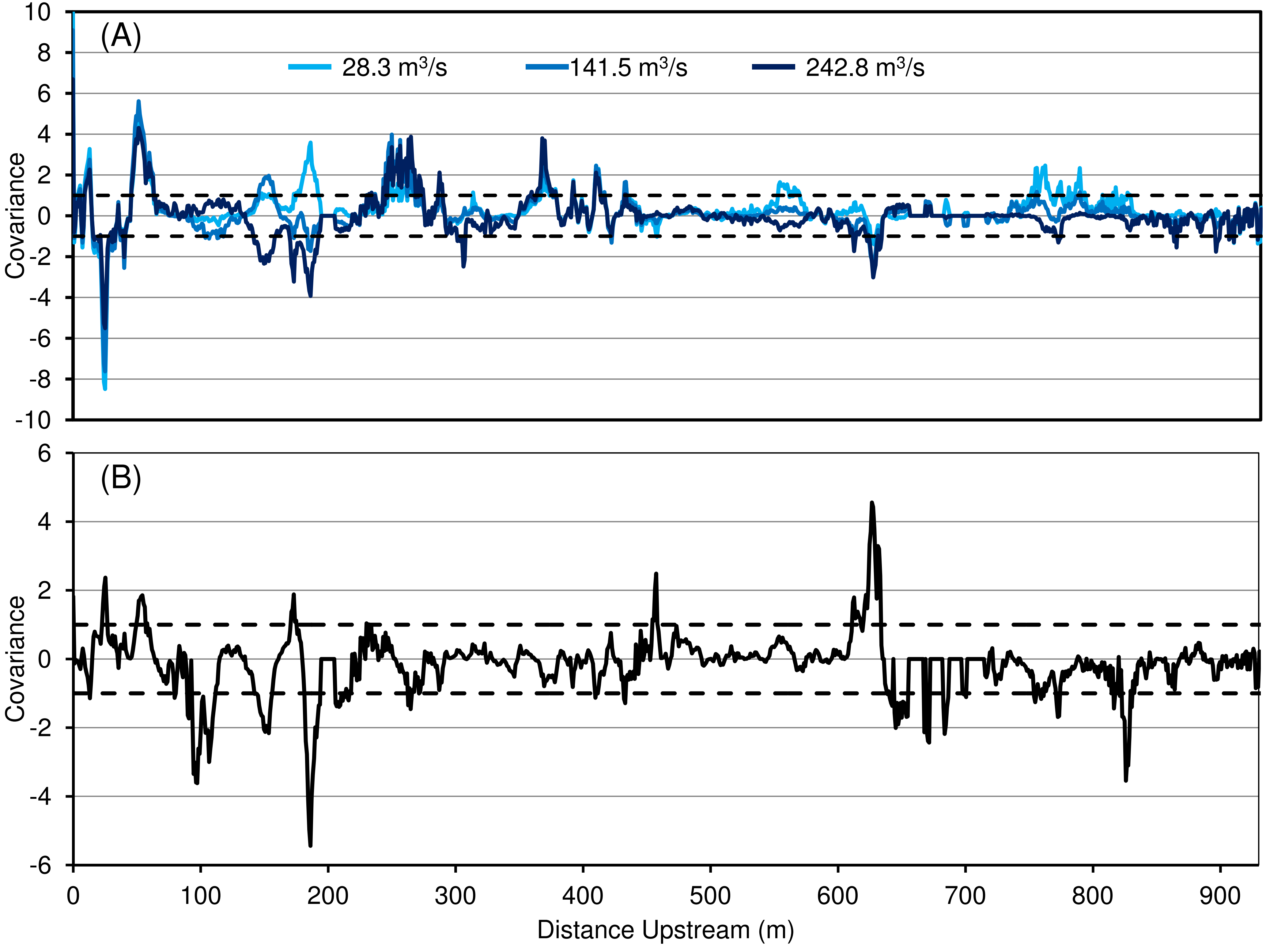

(A)
28.3 m³/s
141.5 m³/s
242.8 m³/s
Covariance
10
8
6
4
2
0
-2
-4
-6
-8
-10
(B)
Covariance
6
4
2
0
-2
-4
-6
0
100
200
300
400
500
600
700
800
900
Distance Upstream (m)

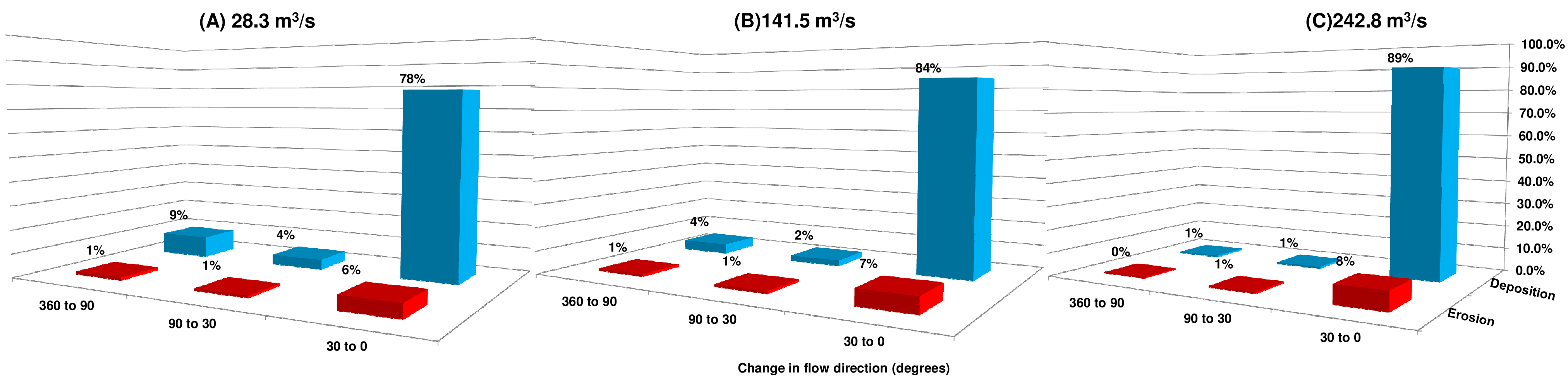
(A) 28.3 m3/s
(B)141.5 m3/s
(C)242.8 m3/s
78%
9%
1%
4%
1%
6%
84%
4%
1%
2%
1%
7%
89%
1%
0%
1%
1%
8%
360 to 90
90 to 30
30 to 0
Change in flow direction (degrees)
Deposition
Erosion
100.0%
90.0%
80.0%
70.0%
60.0%
50.0%
40.0%
30.0%
20.0%
10.0%
0.0%

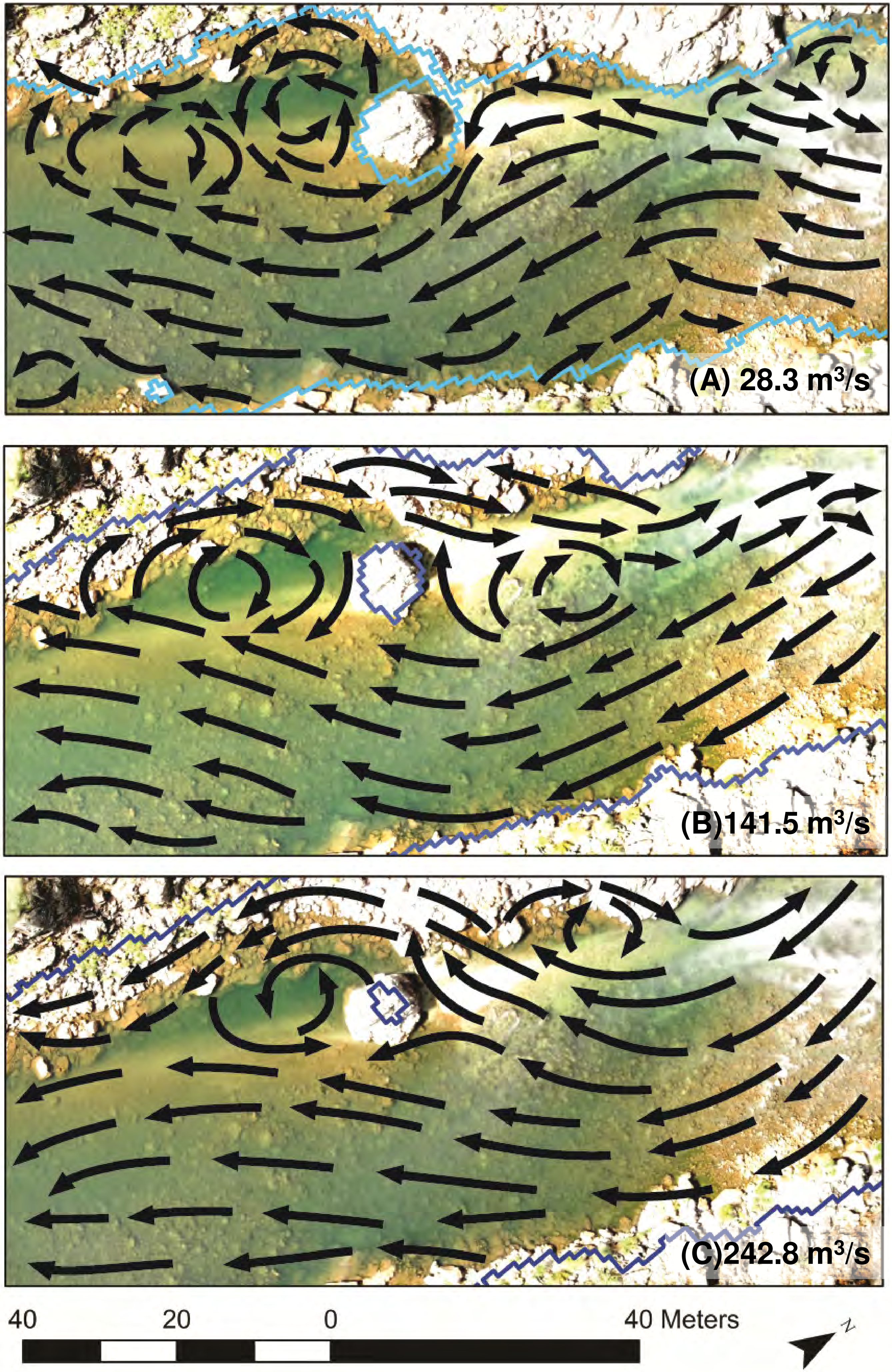
(A) 28.3 m³/s
(B)141.5 m³/s
(C)242.8 m³/s
40
20
0
40 Meters
N

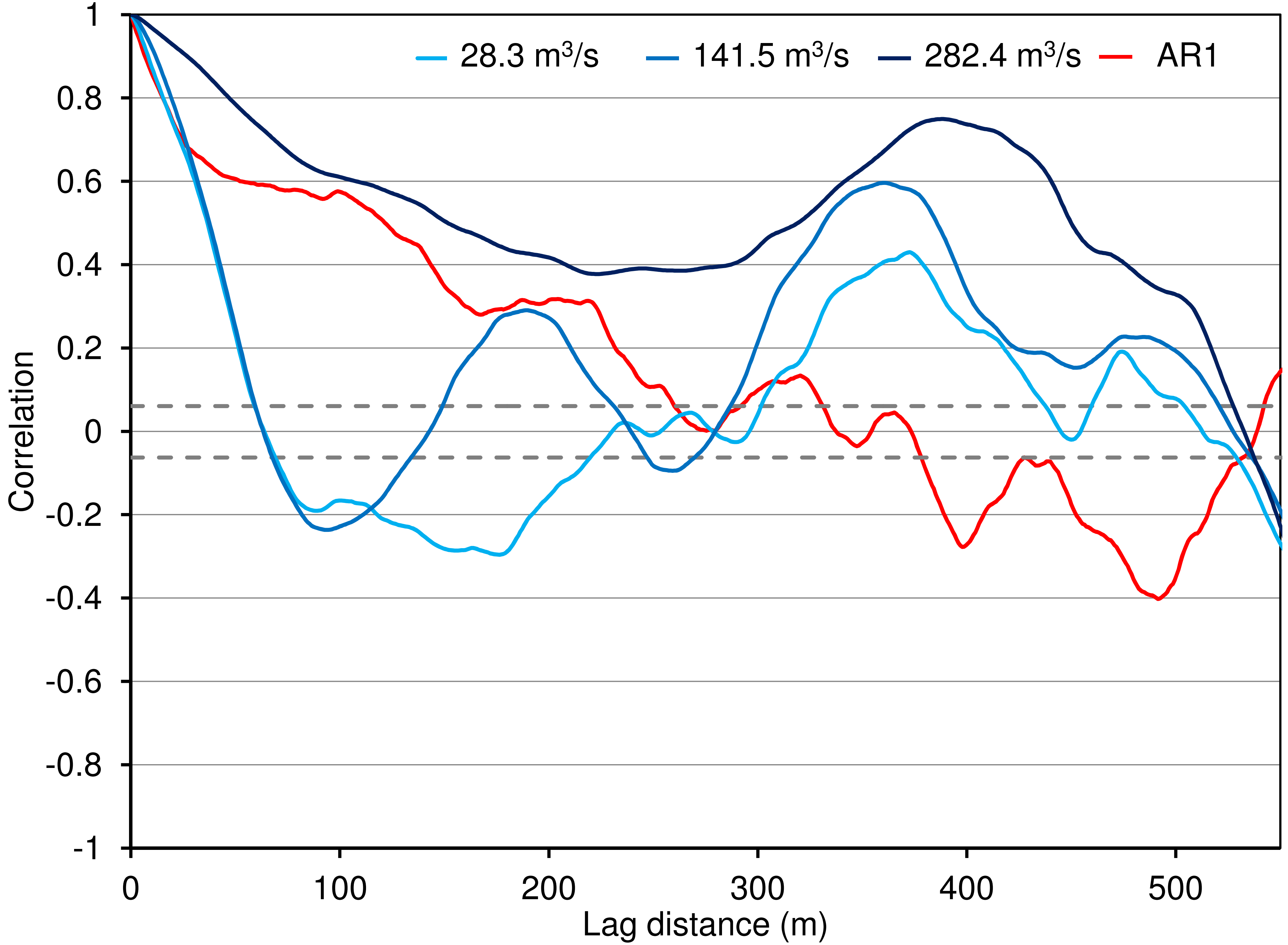
28.3 m³/s
141.5 m³/s
282.4 m³/s
AR1
Correlation
Lag distance (m)
1
0.8
0.6
0.4
0.2
0
-0.2
-0.4
-0.6
-0.8
-1
0
100
200
300
400
500

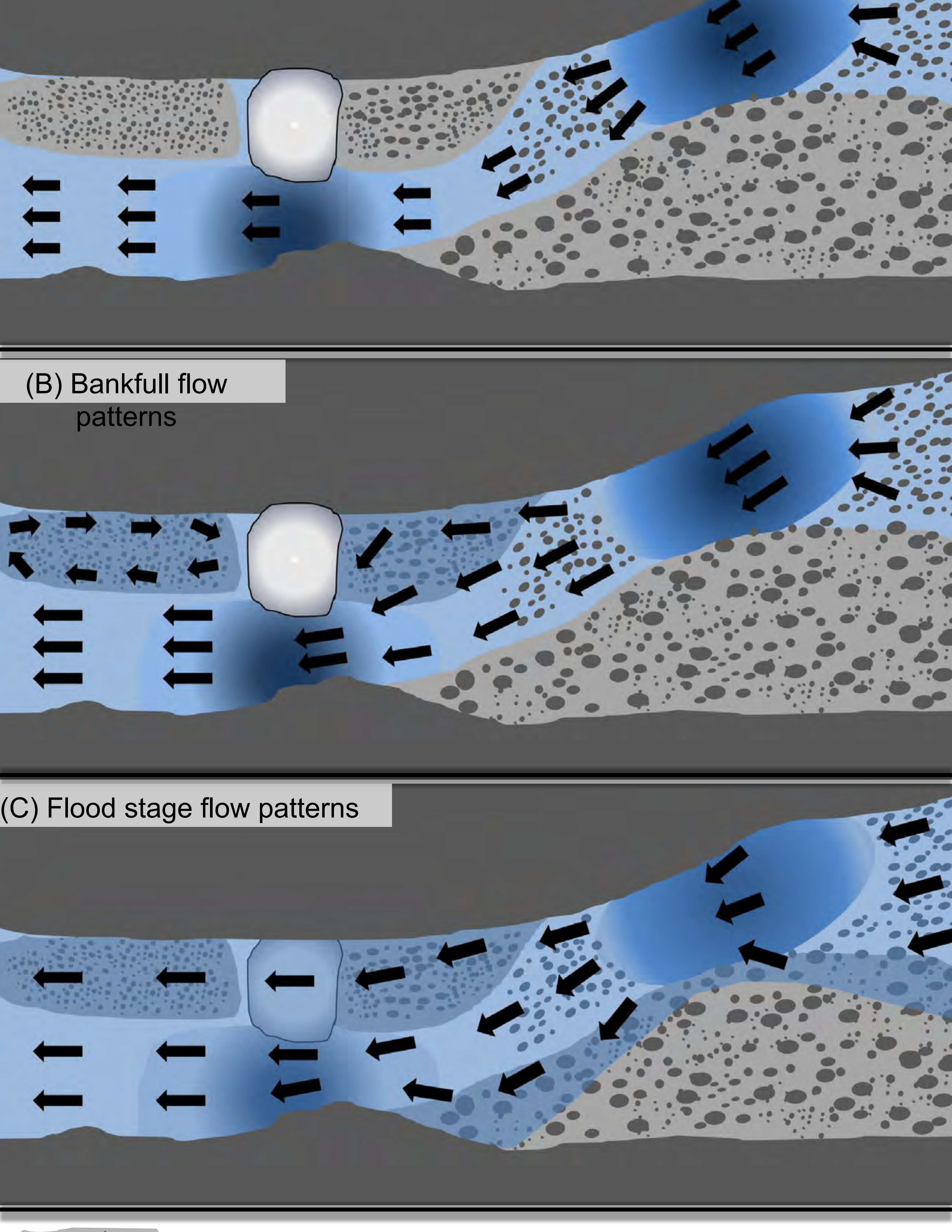
(B) Bankfull flow
patterns
(C) Flood stage flow patterns